communications earth & environment

ARTICLE

https://doi.org/10.1038/s43247-023-01017-8 OPEN

Climate-driven 21st century Caspian Sea level decline estimated from CMIP6 projections

Rohit Samant [1]✉ & Matthias Prange [1,2]✉

Future Caspian Sea level change is estimated for the 21st century using 15 Coupled Model Intercomparison Project 6 climate models and three shared socioeconomic pathways. Projected evaporation increase is significantly larger than precipitation increase integrated over the Caspian Sea catchment basin, resulting in an increasingly negative water balance over the 21st century. A best-fit model analysis that resolves important model limitations related to spatial resolution, climate sensitivity, and Caspian Sea surface area suggests climate-driven sea level reductions of about 8 (inter-model range from 2 to 15) m and 14 (inter-model range from 11 to 21) m by the end of this century for the SSP245 and SSP585 scenarios, respectively. A sea level decline of these magnitudes will result in complete desiccation of the northern Caspian basin and will have adverse effects on ecosystems, coastal infrastructure, navigation, biodiversity, and economies of the entire Caspian region.

[1] Department of Geosciences, University of Bremen, 28359 Bremen, Germany. [2] MARUM—Center for Marine Environmental Sciences, University of Bremen, Leobener Str. 8, 28359 Bremen, Germany. ✉email: rosamant@uni-bremen.de; mprange@marum.de

In the past decades, glacier melting and thermal expansion of the ocean has caused a significant rise in the global sea level. Political and public awareness of this issue was raised by numerous scientific studies and reports of the Intergovernmental Panel on Climate Change (IPCC). As a consequence, adaptation measures are undertaken in many regions to tackle the problem of sea-level rise[1]. On the other hand, there is a lack of political and public awareness on the declining water levels of landlocked seas and lake systems across the world[2]. Increasing temperatures will result in drying up of the continents and an intensified shrinking of lakes in many regions. Endorheic basins, which lack outflows and usually lie in climatic zones that experience arid to semi-arid conditions[3], are particularly vulnerable to climatic change as their water budget is predominantly maintained by precipitation (P) and evaporation (E) fluxes, groundwater exchanges, and inflow by streams and runoff[4,5]. Small variations in these fluxes over a long-term scale can affect the sensitive balance of the water budget and hence the endorheic lake levels. Perturbations can be further magnified by human activities as in the well-documented cases of the desiccated Aral Sea and the shrinking Great Salt Lake[3]. Since the endorheic Caspian Sea lies in the semi-arid zone and is the largest lake in the world with a unique biota, the impacts of Caspian Sea Level (CSL) changes on the five littoral countries can be more devastating than in smaller lake systems. Hence, it is important to understand how large lake systems like the Caspian will behave over the 21st century under global warming conditions.

The Caspian Sea experienced a sharp drop in water level of 1.8 m in the 1930s which continued slowly until the year 1977, resulting in a total decline of 3 m[6,7]. This sea-level drop has been partly linked to the decrease in the precipitation over the Volga catchment region and partly to intense reservoir construction activities on the Volga River[8]. This period was followed by an increase in sea level until the year 1995, which was suggested to be linked to the hydroclimatic effect of an El Nino-Southern Oscillation teleconnection[9]. CSL changes studied by ref. [10] through satellite altimetry highlight a drop in the water level by nearly 7 cm/year for the period 1996–2015, which is nearly about 1.5 m in total. This decline has slightly intensified in recent years resulting in a 10 cm/year drop between 2006 and 2021. The decrease in the water level has desiccated the sea area by ~15,000 km^2, affecting a large portion of the north-east coastal region[11], changing it from a perennial to a seasonal water body[12]. Increased evaporation rates over the Caspian Sea have been suggested to play a dominant role in the recent shrinking of the lake[10].

In light of the magnitude of CSL response during the 20th century when climatic fluctuations resulted in 2–3 m of rise and fall in water levels, it is vital to determine the impact and role of anthropogenic climate change[13]. It is important to understand whether observed sea level trends will continue or even intensify with an increase in atmospheric greenhouse gas concentrations. To estimate future trends in CSL, climate models providing projections are essential.

Though a number of studies have focused on estimating future CSL changes using regional and global climate models, there is still a large discrepancy among projected changes for the 21st century[13–20]. While stable conditions or increasing CSL were suggested by refs. [21,22], most of the other studies proposed a decline in CSL by the year 2100. A CSL drop of 4.5–5 m by the year 2100 was suggested by refs. [13,18], while a recent study[23] estimated a decline of 9–18 m mainly due to increasing lake evaporation. A recent multi-model study[8] using different climate change scenarios from Coupled Model Intercomparison Project (CMIP) experiments projected a CSL decline of up to 8–10 m based on CMIP5 models and up to 20–30 m based on CMIP6 models. However, some of the models (particularly CMIP5 models) included in the study[8] had inaccurate Caspian Sea surface areas, introducing errors in the hydrological budget[24,25]. Moreover, the lake-level equation used in ref. [8] did not account for climate model biases, which likely affected the simulated water budgets (P–E) in the Caspian catchment area and hence the lake-level estimates.

Here, we present a new multi-model approach to project 21st century CSL changes. In order to determine how the hydroclimate of the Caspian catchment region potentially changes in the future, 15 state-of-the-art CMIP6 models were analyzed. This study focuses on estimating the future trend of the CSL by considering climate models that accurately represent the present-day Caspian Sea area and regional climate. The models have been selected for final analysis only if they have high spatial resolution (in the order of 100 km), good skill in simulating the regional climate, and realistic climate sensitivity. The goal of our assessment is to provide a key scientific framework for potential sustainable adaptation strategies. To this end, the following research questions are addressed: (i) How will the hydroclimate in the Caspian Sea catchment region change over the 21st century under three Shared Socioeconomic Pathway (SSP) scenarios—SSP126, SSP245, and SSP585? (ii) How will changes in precipitation and evaporation influence the CSL? (iii) What is the relation between the global temperature increase and changes in the temperature and evaporation in the Caspian catchment basin?

Study area. The Caspian Sea is surrounded by the Russian and Kazakh lowlands in the north, central Asian plateaus and the Karakum Desert in the east, the Elburz mountains in the south, and the Caucasian mountains in the west (Fig. 1). The area of the Caspian catchment basin (~3.7×10^6 km^2) is about 10 times larger than the Caspian Sea surface area[9,23]. The area and volume of the Caspian Sea are ~389,000 km^2 (including ~18,000 km^2 area of the Kara-Bogaz-Gol Bay located to the east of the sea) and ~78,000 km^3, respectively[26]. The catchment area extends from 32°N to 61°N. This vast latitudinal expanse of the catchment basin results in a complex climatological setting and seasonal variability of precipitation patterns in the northern and the southern catchment regions[23]. The northern part of the catchment area, which includes the Volga River basin, receives maximum precipitation in summer[16]. The southern part and the Kura/Terek basin which lies on the western part of the catchment area receive maximum precipitation in autumn-winter and springtime, respectively[27]. The eastern part is a desert and receives limited precipitation[23]. Today, river water east of the Karakum Desert in Turkmenistan evaporates and seeps away. The northern basin of the Caspian freezes in the winter, with the sea-ice covering 20,000–95,000 km^2 (ref. [28]).

On the basis of its bathymetry, the Caspian Sea can be divided into three sub-basins[7]. A shallow (5–10 m deep) northern sub-basin, which is the continuation of the North Caspian plain is separated from the middle sub-basin by the Mangyshlak sill and acts as a shelf break of the basin[24,29]. The middle sub-basin has a maximum depth of 788 m and is separated from the southern sub-basin by the Aspheron Sill[29,30]. The deeper southern basin has a maximum depth of 1052 m (ref. [31]). The Caspian Sea is fed by about 130 rivers with the Volga River being the most significant supplier to the Caspian Sea[27]. The Volga River discharges into the northern shelf and contributes ~80–90% of the total runoff to the Caspian Sea[7].

Results

CMIP6 model performance and skills. For our analysis, 15 models from 13 institutions were used (see Methods; Table 1).

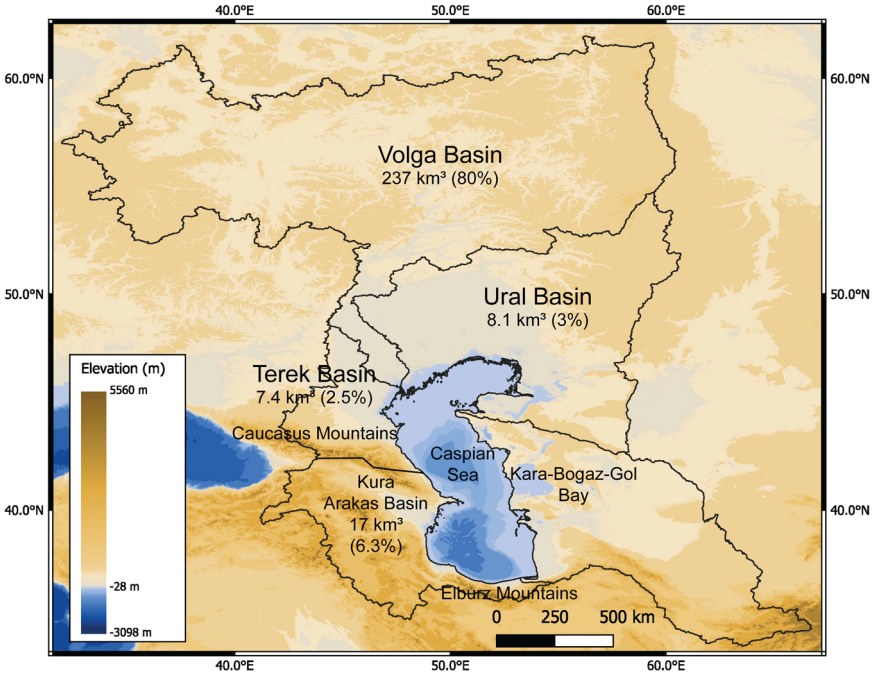

Fig. 1 Drainage basin and sub-basins of the Caspian Sea. Annual discharge data from ref. [7] and bathymetry data acquired from GEBCO Compilation Group (2022) GEBCO 2022 Grid (https://www.bodc.ac.uk/data/published_data_library/catalogue/10.5285/e0f0bb80-ab44-2739-e053-6c86abc0289c).

Table 1 CMIP6 models used in this analysis.

Models	Institution	Resolution	Historical *P-E* mean	Caspian Sea implementation	Exclusion method/best fit model
AWI-CM-1-1-MR	Alfred Wegener Institute, Germany[41]	0.9° x 0.9°	0.025	Lake	Best fit model
BCC-CSM2-MR	Beijing Climate Center, China[42]	1.12° x 1.12°	0.097	Lake	Best fit model
CAMS-CSM-1-0	Chinese Academy of Meteorological Sciences, China[43]	1.12° x 1.12°	0.095	Lake	ECS; Taylor diagram—precipitation and evaporation
CMCC-CM2-SR5	Euro-Mediterranean Center on Climate Change, Italy[44]	0.9° × 1.25°	−0.045	Ocean	Caspian Sea surface area
EC-Earth3	Earth Consortium, Rossby Center,	0.7° x 0.7°	−0.052	Lake	ECS; Taylor diagram—
EC-Earth3-Veg	Sweden[45]	0.7° x 0.7°	−0.051	Lake	evaporation
FGOALS-f3-L	Chinese Academy of Sciences, China[46]	1.0° x 1.0°	0.314	Lake	Taylor diagram—evaporation
FIO-ESM-2-0	First Institute of Oceanography, China[47]	0.9° × 1.25°	0.001	Ocean	Caspian Sea surface area
GFDL-ESM4	NOAA, Geophysical Fluid Dynamics Laboratory, USA[48]	1.25° x 1.0°	0.136	Lake	Best fit model
INM-CM4-8	Institute of Numerical Mathematics,	1.5° x 2°	0.031	Ocean	ECS; Model resolution
INM-CM5-0	Russian Academy of Science, Russia[49, 50]	1.5° x 2°	0.096	Ocean	
MPI-ESM1-2-HR	Max Planck Institute for Meteorology, Germany[51]	0.9° x 0.9°	0.095	Lake	Best fit model
MRI-ESM2-0	Meteorological Research Institute, Japan[52]	1.12° x 1.12°	0.285	N/A	Taylor diagram—evaporation
NorESM2-MM	Norwegian Climate Center, Norway[53]	1.25° × 0.9°	0.102	Lake	Best fit model
TaiESM1	Research Center for Environmental Changes, Academia Sinica (Taiwan)[54]	1.25° × 0.9°	0.015	Ocean	ECS; Caspian Sea surface area

Historical catchment-averaged *P–E* means in mm/day are calculated for the period 1850–2014. Exclusion method summarizes the criteria applied to select CMIP6 models for best fit model analysis.

Taylor diagrams are particularly suitable for assessing the relative skill of multiple models or in evaluating various facets of complex models[32]. To assess the skill of the CMIP6 models in simulating the Caspian regional climate, the period 1979–2008 from the historical simulations was validated against European Centre for Medium-Range Weather Forecasts reanalysis (ERA5) data using Taylor diagrams. The Taylor diagram (Fig. 2a) shows that most of the CMIP6 models have spatial correlation values with respect to ERA5 of <0.8 for annual evaporation (including sublimation and transpiration) in the Caspian region. Models such as CMCC-CM2-SR5, FIO-ESM-2-0, and TaiESM1 show relatively low skill (low spatial correlation) which can be linked to the representation of the Caspian Sea in these models. These three models set the CSL to the global sea level (0 m) instead of −28 m. This results in a larger surface area of the Caspian Sea, especially over the North Caspian basin. A larger surface area of the Caspian Sea also results in a positive bias in the model simulations, as most of the evaporation takes place over the Caspian Sea surface. Along with these low skills, FGOALS-f3-L and INM-CM5-0 also show low normalized standard deviation values. Two models (EC-Earth3

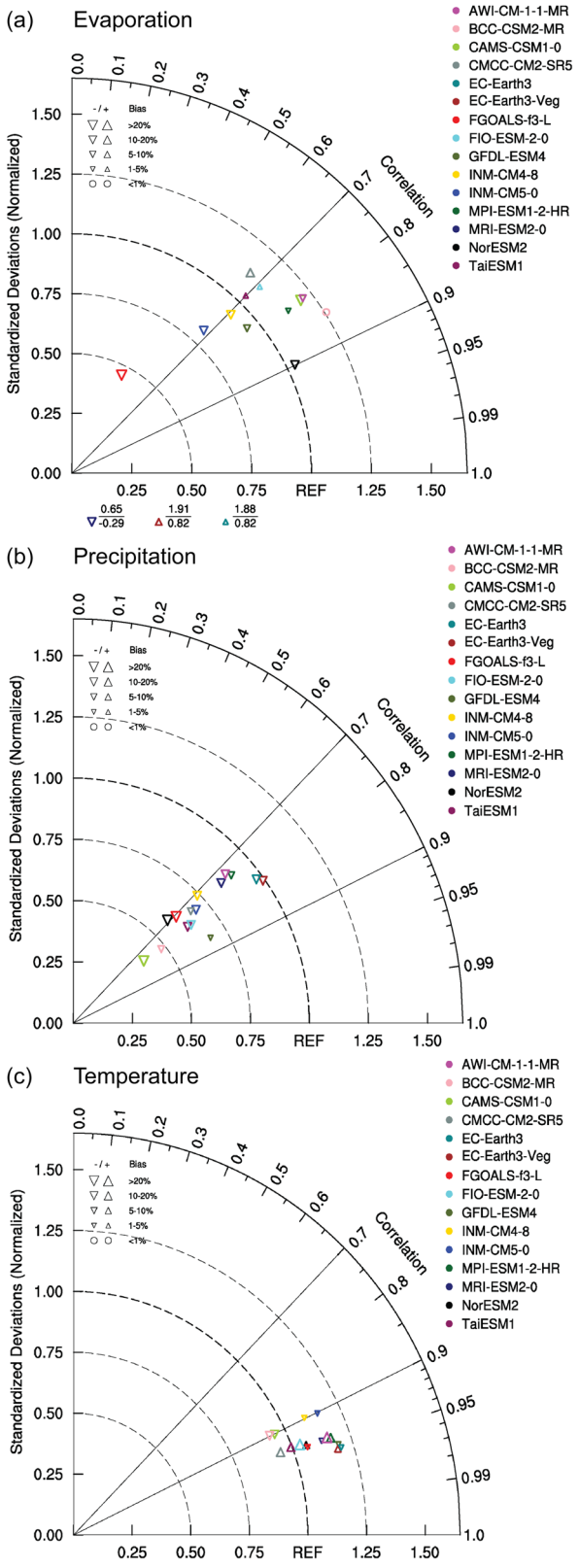

Fig. 2 Taylor diagram for evaporation, precipitation and temperature (annual means) over the Caspian region (36–60°N, 45–55°E) for 15 CMIP6 model simulations and ERA5 reference data for the time period 1979–2008. a Evaporation, (**b**) precipitation and (**c**) temperature. The diagram indicates the normalized standard deviations on the radius and the spatial correlation on the angular axis. The markers indicate the sign and percent bias for the models.

and EC-Earth3-Veg) have a normalized standard deviation >1.65. MRI-ESM2-0 has a negative spatial correlation for evaporation. AWI-CM-1-1-MR, BCC-CSM2-MR, CAMS-CSM1-0, and MPI-ESM1-2-HR display better skills for simulating evaporation; however, they overestimate the standard deviation. In comparison to other models, GFDL-ESM4 and NorESM2-MM quite accurately simulate evaporation in the Caspian region.

All 15 CMIP6 models on comparison with the ERA5 data, show spatial correlation between 0.7 and 0.9 for annual precipitation (Fig. 2b). Most of the models and especially BCC-CSM2-MR and CAMS-CSM1-0 underestimate the standard deviation of precipitation in the Caspian region. While models such as AWI-CM-1-1-MR and MPI-ESM1-2-HR show a slight underestimation of the standard deviation in the simulation of precipitation, EC-Earth3 and EC-Earth3-Veg accurately estimate the precipitation over the Caspian region. Except for GFDL-ESM4, all the models show significant negative bias in the simulation of precipitation. The negative bias can be partly linked to the disability of the models to accurately simulate orographic precipitation in the mountainous regions of the Caucasus and Elburz (Supplementary Fig. 1). Based on this analysis, it can be suggested that model resolution of at least 0.7° is required to reasonably simulate precipitation over the mountainous regions.

The CMIP6 models show better skills (high spatial correlation) in the simulation of 2 m surface air temperature (T2m) over the catchment region of the Caspian Sea (Fig. 2c). BCC-CSM2-MR, CAMS-CSM1-0, and CMCC-CM2-SR5 display a slight underestimation of the standard deviation in the simulation of T2m. TaiESM1 accurately simulates T2m in the catchment region with a positive bias. Many CMIP6 models show an overestimation in simulating T2m. While FGOALS-f3-L shows the lowest bias, FIO-ESM-2-0 and AWI-CM-1-1-MR show large positive biases.

Projected water budget changes of the Caspian Sea catchment basin. Linear trends of catchment-averaged precipitation, evaporation, and *P–E* were calculated, which represent the projected 21st century long-term evolution (2020–2100) for the different pathway scenarios, viz SSP126, SSP245, and SSP585 (note that throughout this paper the term catchment basin refers to the entire Caspian catchment area, including the land catchment and the Caspian Sea surface). Although the results show a general tendency towards increasing precipitation with warmer climates, several models show different behavior (Fig. 3a). Some models like AWI-CM-1-1-MR and BCC-CSM2-MR show a significant drop in precipitation for the SSP585 scenario. Unlike precipitation, evaporation shows a more homogeneous behavior with more-or-less increasing evaporation trends in response to an increase in warming, although exceptions also exist (Fig. 3b). Evaporation increases substantially with rise in warming from SSP126 to SSP585 scenarios in most models. CMCC-CM2-SR5, EC-Earth3, and EC-Earth3-Veg show the strongest rise in evaporation.

P–E trends determine changes in CSL and are therefore of particular relevance for this study (Fig. 3c). Except for FGOALS-f3-L and INM-CM4–8, all models show negative *P–E* trends for two or more pathway scenarios. Though there is no clear trend of stronger negative P–E trends with an increase in warming, it is quite evident that evaporation dominates over precipitation irrespective of the pathway scenario (Fig. 3c).

Supplementary Table 1 shows the *P–E* trends (2020–2100) for the 15 CMIP6 models and the different pathway scenarios. Considering all the 15 CMIP6 models, the mean of *P–E* trends for SSP126, SSP245 and SSP585 are −0.016, −0.027 and −0.051 mm/day/81 years, respectively while the inter-model standard

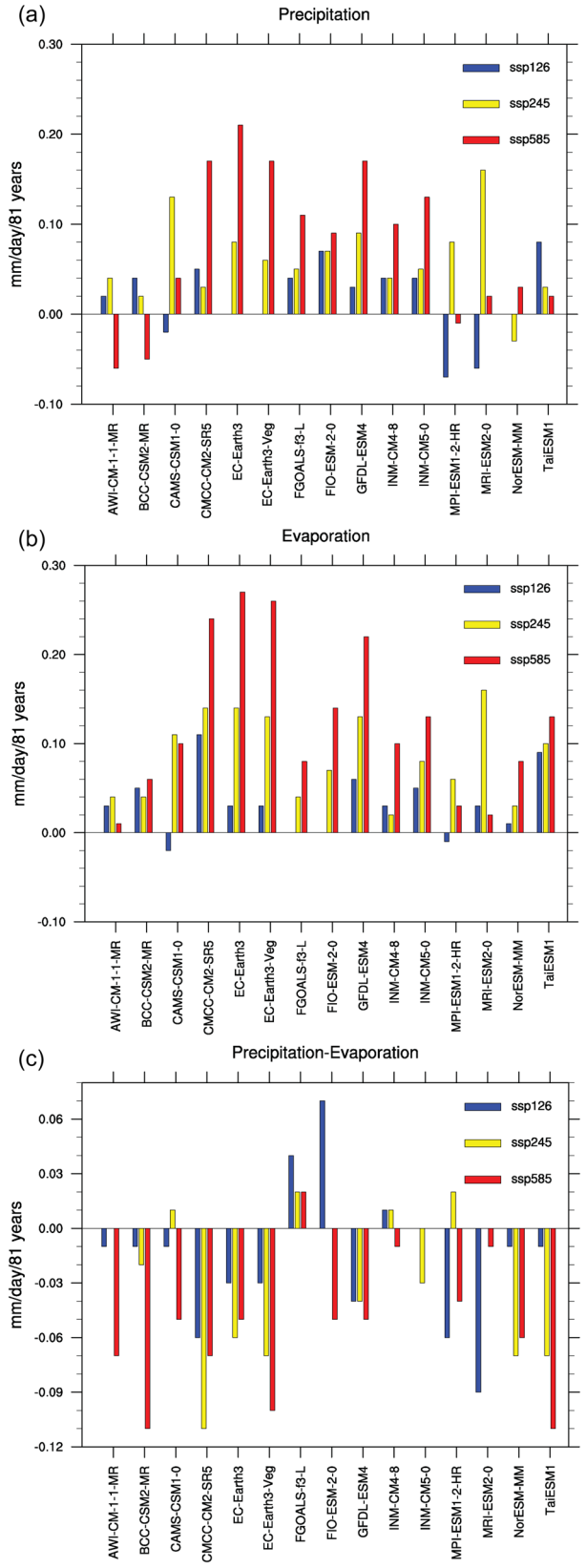

Fig. 3 Bar plots showing projected precipitation, evaporation and precipitation-evaporation trends based on linear trend analysis of annual means (2020–2100) averaged over the Caspian catchment basin for 15 CMIP6 models. a Precipitation, (**b**) evaporation and (**c**) precipitation-evaporation trends. Colors indicate SSP126 (blue), SSP245 (yellow), and SSP585 (red).

deviations of *P*–*E* trends for SSP126, SSP245 and SSP585 are 0.038, 0.039 and 0.037 mm/day/81 years, respectively. Multi-model mean catchment-averaged *P*–*E* shows significantly ($p < 0.05$) decreasing trends (-0.0152 ± 0.0145 mm/day/81 years for SSP126, -0.0269 ± 0.0128 mm/day/81 years for SSP245 and -0.0504 ± 0.0158 mm/day/81 years for SSP585) for the time period 2020–2100 (Supplementary Fig. 2). The CSL change (ΔCSL) can be estimated from these *P*–*E* trends on the basis of a simple water budget equation ("bathtub model" analogous to ref. [16]):

$$\Delta \mathrm{CSL} = A_T/A_S \cdot \Delta[P-E]/2 \cdot \Delta t, \quad (1)$$

where A_T/A_S is the ratio of the total area of the Caspian catchment basin to the Caspian Sea surface area and is approximately equal to 10, $\Delta[P–E]$ is the linear trend of catchment-averaged *P*–*E* per 81 years, and Δt is the considered time period equal to 81 years. This approach only considers the projected long-term trend in the Caspian Sea water budget and hence requires no assumptions regarding the present water balance. Applying Eq. (1), the above *P*–*E* trends translate into a CSL drop of 2.25 ± 2.14 m for the SSP126 scenario, 3.97 ± 1.89 m for the SSP245 scenario, and 7.45 ± 2.33 m for the SSP585 scenario.

In order to further elucidate how the regional hydroclimate change relates to temperature rise, linear trends of catchment-averaged annual mean *P*, *E*, and *P*–*E* for SSP126, SSP245, and SSP585 were plotted against catchment-averaged annual mean T2m 2020–2100 trends (Fig. 4). While precipitation shows a significantly ($p < 0.05$) increasing trend of 0.011 ± 0.008 mm/day/81 years per 1 °C/81 years warming, evaporation significantly ($p < 0.05$) increases by 0.020 ± 0.007 mm/day/81 years per 1 °C/81 years rise (Fig. 4a, b). A significantly ($p < 0.05$) decreasing trend of -0.009 ± 0.005 mm/day/81 years per 1 °C/81 years for *P*–*E* emphasizes the dominance of evaporation over precipitation over the entire Caspian catchment basin (Fig. 4c). Trends of evaporation over the Caspian Sea surface against catchment-averaged T2m trends show a significantly ($p < 0.05$) positive trend of 0.070 ± 0.014 mm/day/81 years per 1 °C/81 years (Fig. 4d). This value suggests that warming-induced changes in evaporation fluxes over the Caspian Sea are 3-4 times larger than over the entire catchment region, underlining how this evaporation component is an important factor for the hydrological budget of the Caspian catchment region. Regression analysis of catchment-averaged T2m trends against global T2m trends show a significantly ($p < 0.05$) positive slope of 1.4 ± 0.1, indicating amplified warming of the Caspian Sea catchment region over the 21st century (Supplementary Fig. 3a). Catchment-averaged *P*–*E* trends against global T2m trends show a significantly ($p < 0.05$) decreasing trend of -0.013 ± 0.007 mm/day/81 years per 1 °C/81 years (Supplementary Fig. 3b). This trend suggests that the CSL will drop by 1.9 ± 1.0 m for each 1 °C global temperature rise by the end of the century.

Best-fit analysis. In the previous section, all available CMIP6 models were considered in our analysis of future CSL change without taking their skills into account. In the following, we select best-fit models on the basis of model simulation skills by means of the Taylor diagrams, Caspian Sea surface representation, and equilibrium climate sensitivity (ECS) to further constrain estimates of future CSL change.

The Taylor diagrams offer statistics to analyze the models' performance for individual climatological variables and thus evaluate the model skills to simulate the hydroclimate of the Caspian region. We consider models with low skill as less

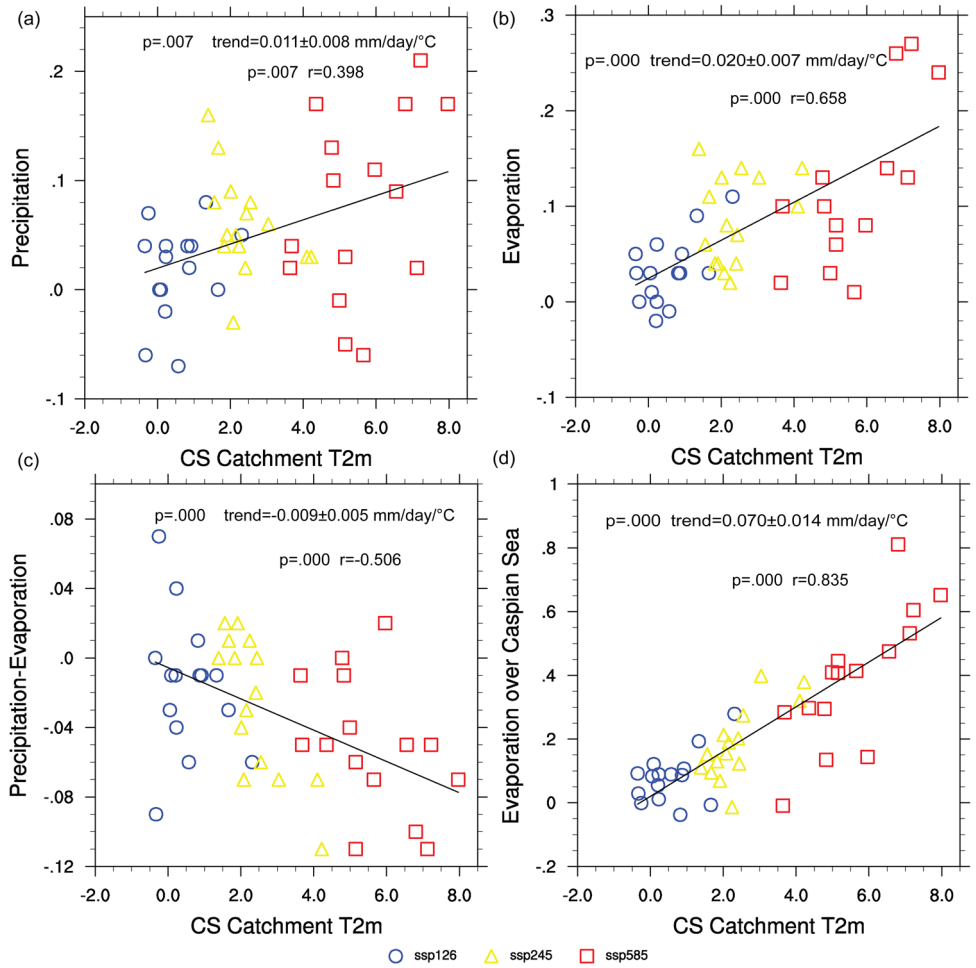

Fig. 4 Annual mean (2020–2100) catchment-averaged trends of precipitation (mm/day/81 years), evaporation (mm/day/81 years), *P–E* (mm/day/81 years), and evaporation (mm/day/81 years) over the Caspian Sea against catchment-averaged T2m trends (°C/81 years) for all the 15 CMIP6 models and 3 scenarios. a Precipitation, (**b**) evaporation, (**c**) *P–E*, and (**d**) evaporation over the Caspian Sea. Trend values are provided with 95% confidence interval for the trend analysis. *r* and *p* give the correlation coefficient and *p*-value, respectively.

trustworthy to simulate future changes in the Caspian Sea regional hydroclimate. Therefore, based on these statistics, some of the CMIP6 models were not included in the best-fit model analysis. CMIP6 models were excluded if one of the climatological variables displays an outlier in the Taylor diagrams. Clear outliers were identified by negative spatial correlation and too high standard deviation. While EC-Earth3 and EC-Earth3-Veg show outliers due to high standard deviation in evaporation, MRI-ESM2-0 indicates an outlier due to negative spatial correlation (Fig. 2a).

Accurate representation of the Caspian Sea surface in the models is an essential factor for precise estimation of the water budget over the Caspian Sea catchment basin as the evaporation over the Caspian Sea surface is an important component of the hydrological budget (Fig. 4d). Some CMIP6 models such as FIO-ESM-2-0, CMCC-CM2-SR5, and TaiESM1 set the CSL to the global sea level (0 m) instead of −28 m. As a consequence, evaporation over the sea surface takes place from a larger surface area than the actual surface area (Supplementary Fig. 4a–c) and results in a potential overestimation of future evaporation trends from the Caspian Sea surface (Fig. 5a–c). For this reason, none of these three models were taken into consideration for the best-fit analysis.

While some models overestimate evaporation over the Caspian Sea surface, the Caspian Sea appears to be neglected in MRI-ESM2-0 (Supplementary Fig. 5b). As a result, the *P–E* trend analysis is lacking the evaporation component over the Caspian Sea surface (Fig. 5e) and hence, this model was excluded from the best-fit analysis. Unlike MRI-ESM2-0, FGOALS-f3-L accurately represents the area of the Caspian Sea surface. Nevertheless, this model shows low skill in simulating the regional evaporation field and represents a clear outlier from the rest of the models in the evaporation Taylor diagram (Fig. 2a, Supplementary Fig. 4d). This also affects the *P–E* linear trend map projection, where a substantial underestimation of negative *P–E* is observed over the Caspian Sea when compared with other model simulations (Fig. 5f). By contrast, EC-Earth3 and EC-Earth3-Veg appear to overestimate evaporation over the Caspian Sea surface (Supplementary Fig. 5c, d), which is reflected in the *P–E* trends over the southern Caspian Sea (Fig. 5d).

Equilibrium climate sensitivity (ECS) is a measure of the increase in the global temperature for a doubling of CO_2 concentrations above pre-industrial levels. Many CMIP6 models with ECS values > 4.5 overestimate the recent warming trends and are also likely to overestimate future 21st century warming[33,34]. We therefore consider models with unrealistic ECS less reliable in projecting future Caspian regional climate. ECS values were acquired from ref. [35] to determine how many CMIP6 models applied in this work fit the IPCC AR6 likely range of 2.5 °C to 4.0 °C. Models like EC-Earth3, EC-Earth3-Veg, CMCC-CM2-SR5

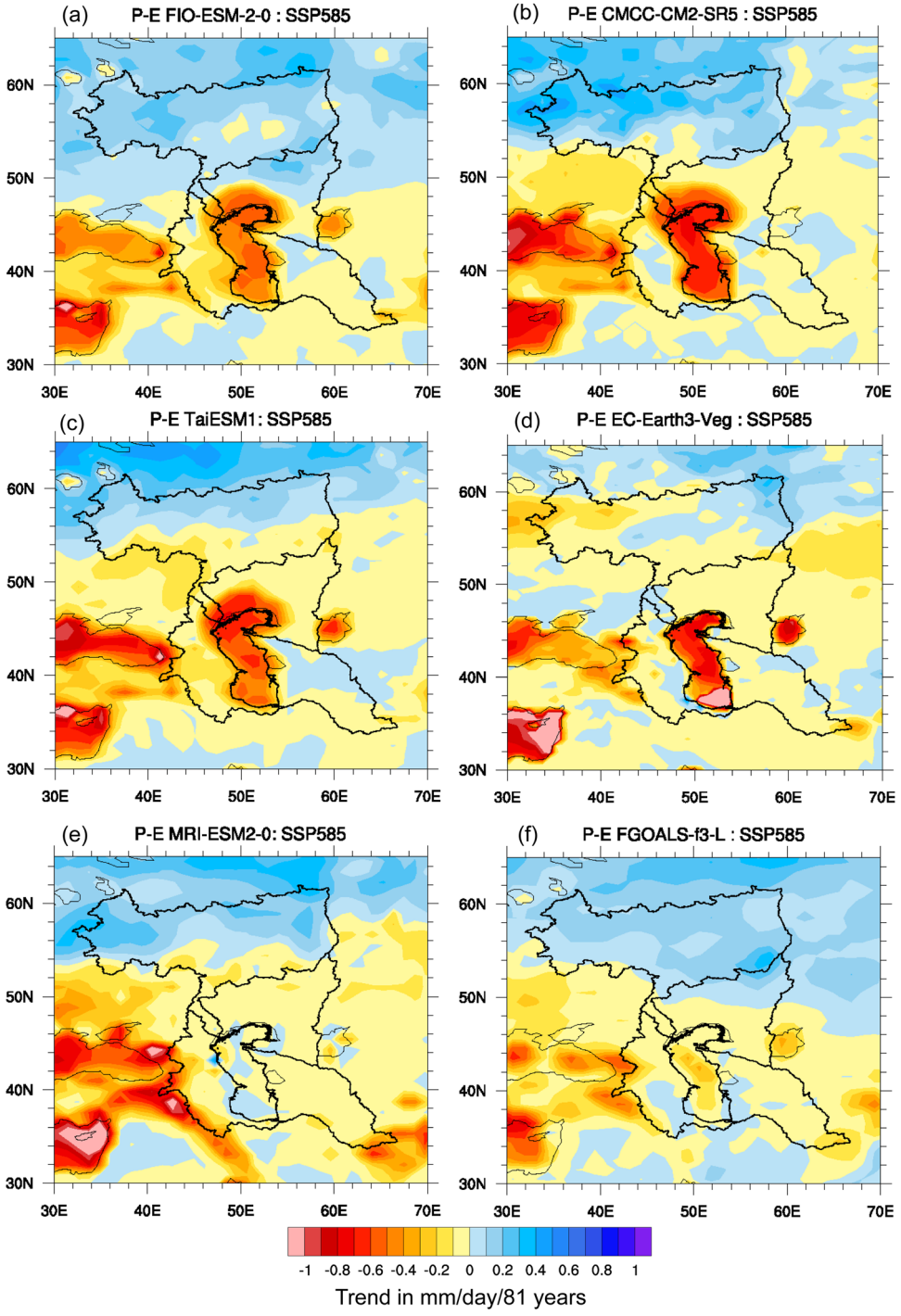

Fig. 5 Linear trends of annual means of P–E for SSP585 projected by different models. a FIO-ESM-2-0, (**b**) CMCC-CM2-SR5, (**c**) TaiESM1, (**d**) EC-Earth3-Veg, (**e**) MRI-ESM2-0, and (**f**) FGOALS-f3-L for the period of 2020–2100. Catchment area is outlined.

and TaiESM1 which show large projected evaporation trends over the Caspian Sea, have relatively high ECS values or above the likely range of IPCC AR6 (Supplementary Fig. 6). On the contrary, CAMS-CSM1-0, INM-CM4–8 and INM-CM5-0 have ECS values below the likely range (Supplementary Fig. 6). In addition, CAMS-CSM1-0 has a low skill in simulating the regional precipitation (Fig. 2c), while the relatively low spatial resolution of 1.5° × 2° in INM-CM4–8 and INM-CM5-0 (Table 1) affects the model performance to simulate precipitation in the mountainous regions of Elburz and Caucasus (Supplementary Fig. 1c, d). Low model resolution also results in an inability to precisely represent the Caspian Sea surface (Supplementary Fig. 4e, f). Given the low ECS along with low model resolution, these models were not included in the group of best-fit CMIP6 models to estimate CSL changes.

On the basis of ECS values, model performance, and the Caspian Sea surface representation, 10 CMIP6 models in total were excluded from the best-fit analysis (Table 1). The remaining five CMIP6 models (AWI-CM-1-1-MR, BCC-CSM2-MR, GFDL-ESM4, MPI-ESM1-2-HR, NorESM2-MM) have ECS values within the IPCC AR6 likely range (Supplementary Fig. 6) and accurately represent the surface area of the Caspian Sea (Supplementary Fig. 7). These

five models also perform better and hence our best-fit model analysis for future CSL change is based on this group. The 2020–2100 timeseries of *P*–*E* based on the annual means averaged over the Caspian catchment basin using the best-fit model-mean shows a decreasing trend of −0.0247 ± 0.0238 mm/day/81 years for SSP126, −0.0257 ± 0.0257 mm/day/81 years for SSP245, and −0.0646 ± 0.0254 mm/day/81 years for SSP585 (Supplementary Fig. 8). These values translate into CSL drops of 3.65 ± 3.51 m for SSP126, 3.79 ± 3.80 m for SSP245, and 9.55 ± 3.75 m for SSP585. Thus, the best-fit model analysis suggests stronger CSL decline for SSP126 and SSP585 scenarios in comparison to estimates based on 15 CMIP6 models.

Projected hydroclimatological changes in the best-fit models. To determine the climatological patterns and changes over the 21st century, map projections over the Caspian region were examined for the SSP585 scenario of the five best-fit CMIP6 models. Precipitation increases in the northern part of the Volga catchment region in all the models (Supplementary Fig. 9). Most of the models show a strong negative trend for precipitation in the western part of the Caspian catchment region. Following precipitation, evaporation also increases considerably in the northern part of the Volga catchment region in all the models (Supplementary Fig. 10). It should be noted that a drop in the evaporation trends does not necessarily imply wetting of the soil but signifies the non-availability of moisture for evaporation in these regions. Moreover, it is important to notice the strong increase of evaporation over the Caspian Sea for the SSP585 scenarios in all the best-fit models. *P*–*E* increases in the northern part of the Volga catchment area due to the increase in precipitation (Fig. 6). However, most other parts of the Caspian catchment region exhibit overall decreasing *P*–*E* trends. The sharp rise of evaporation over the Caspian Sea is obviously reflected in the *P*–*E* trends.

It has been shown previously that the rise in evaporation has primarily thermodynamic causes[23]. The reduction of the Bowen ratio (i.e., the ratio of sensible to latent heat fluxes at the surface) with increasing surface temperatures as a consequence of the Clausius-Clapeyron equation's non-linearity was emphasized in previous studies[36,37]. As a result, more energy is allocated to increase evaporation[37]. In our multi-model context, we want to revisit the single-model based finding[23] that changes in wind speed play no role in the evaporation rise. To this end, we analyze evaporation trends against near-surface wind speed trends in the best-fit model ensemble (Supplementary Fig. 11). We find that evaporation trends over the Caspian Sea and its catchment area generally decrease with increasing wind speed. Due to the negative correlation, we confirm that changing wind speed is not a driver for the projected evaporation increase.

Discussion

Satellite altimetry measurements show a CSL decline of ~1.5 m/26 years in the period 1996–2021 (Fig. 7). The CSL remained stable until 2005 but the decline intensified from year 2006 onward and has resulted in a drop of ~1.4 m/16 years which is a ~9 cm/year decline. If this rate remains constant, the CSL will drop by ~7 m by the end of the 21st century. However, this trend value refers to a short time period of only 16 years which can be strongly influenced by interdecadal variability. The more robust long-term trend over 26 years however still suggests a ~4.6 m drop by the year 2100, if the current water budget remains constant. It is interesting to note that the Caspian catchment-averaged ERA5 mean annual 2 m air temperature has increased by 1.2° ($p < 0.05$) in the period 1996–2021. It is therefore assumed that the recent and current CSL decline results from an imbalance in the water budget caused by the ongoing warming[38].

Despite a long-term CSL decline of ~2 m from year 1850 to 2014 (ref. [10]), most of the CMIP6 historical simulations suggest positive *P*–*E* mean values over the Caspian catchment region for this period due to model biases (Supplementary Fig. 12, Table 1). A main advantage of our approach of estimating CSL changes based on Eq. (1) is that it does not require a bias correction of *P*–*E*, since only trends of *P*–*E* are used, whereas absolute *P*–*E* values do not enter the equation. As this study focuses only on future climate-driven estimates of sea level change (2020–2100), the current rate of CSL decline of 1.5 m/26 years (see above), which corresponds to 5.7 cm/year, has to be added to the future projections.

Our study shows that anthropogenic warming over the 21st century will lead to further perturbations of the Caspian Sea water budget resulting in additional CSL decline on top of the current trend. On the basis of the best-fit model ensemble, linear trend analysis of *P*–*E* suggests 3.79 ± 3.80 m and 9.55 ± 3.75 m of such additional CSL decline by the year 2100 for the SSP245 and SSP585 scenarios, respectively. This will result in a total drop of ~8 (inter-model range from 2 to 15) m and ~14 (inter-model range from 11 to 21) m by the year 2100 for SSP245 and SSP585, respectively which will completely desiccate the northern Caspian basin and the Kara-Bogaz-Gol Bay (Fig. 8). However, if the CSL decline of ~1.4 m/16 years (2006–2021) was considered, the CSL would even drop by ~11 m and ~17 m by the year 2100 for SSP245 and SSP585, respectively. It is important to note that the best-fit model estimate for SSP126 (additional CSL decline of 3.65 ± 3.51 m) is very close to the estimate for SSP245. Mitigating global warming in the SSP126 scenario does little to improve this situation compared to SSP245. Thus, limiting the global temperature rise to <2 °C according to the Paris agreement will likely not be sufficient to prevent a "Caspian catastrophe". Such drastic changes in the CSL will result in substantial ecological and environmental damage[2]. In this case, adverse effects on biodiversity, ecosystems, navigation, and economies of the littoral states can only be alleviated by formulating and implementing coordinated adaptation and mitigation measures.

In the worst-case scenario, the 21st century CSL drop will be much larger than previous estimates[13,15,18], which range between 4.5 m and 9 m, but smaller than the most recent estimates[8,23]. However, estimates from ref. [18] are based on a low-resolution coupled climate model with simplified physics compared to global general circulation models. This resulted in an inaccurate simulation of precipitation in the mountainous regions. Low-resolution of the model allowed for defining only the large river basins and this potentially affected CSL calculations. The estimate by ref. [23] is affected by a too large Caspian Sea surface area in the CESM climate model, which resulted in an overestimation of the evaporation. A wide range of CSL changes from a small increase to a drop of 20 to 30 m by the year 2100 was suggested by ref. [8]. The lake-level equation applied in that study, however, did not account for climate model biases, which can be larger than climate change signals and hence can severely compromise the CSL calculations. The present study is the first one that estimates future CSL change by a best-fit selection of validated models. The best-fit analysis implemented in this study was vital for a more reliable estimation of future CSL changes. Selection of the CMIP6 models on the basis of model resolution and their ability to accurately simulate the regional climate, resolved limitations from previous studies related to low spatial model resolution and orography-related biases. Filtering out models that incorrectly represent the surface area of the Caspian Sea resolved the limitations of overestimation of evaporation over the Caspian Sea observed in other studies[8,23]. Consideration of the ECS filtered

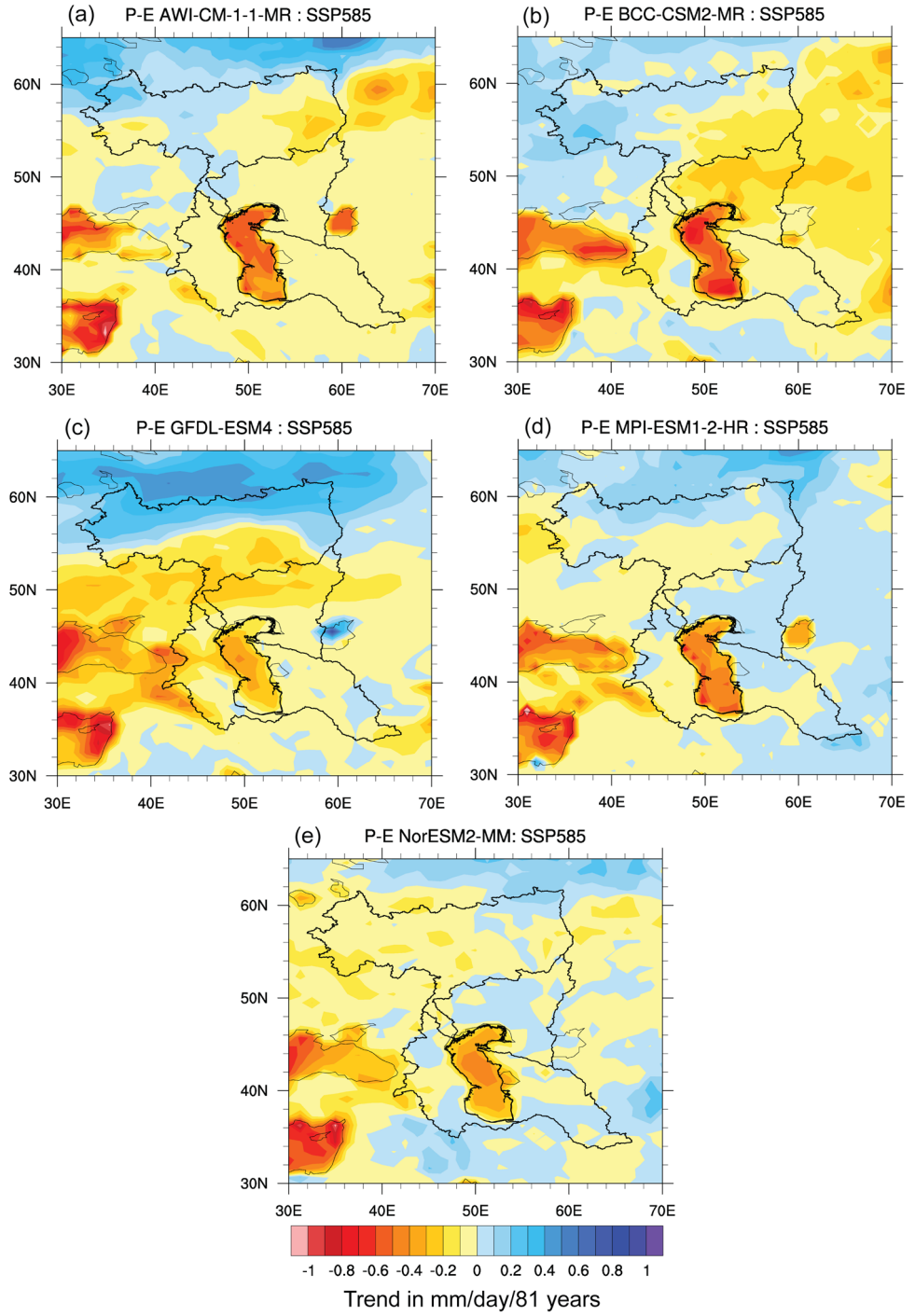

Fig. 6 Linear trends of annual means of *P–E* for SSP585 projected by best-fit models. a AWI-CM-1-1-MR, (**b**) BCC-CSM2-MR, (**c**) GFDL-ESM4, (**d**) MPI-ESM1-2-HR, and (**e**) NorESM2-MM for the period 2020–2100. Catchment area is outlined.

out models that simulate unrealistic climate changes. Hence, reducing important model limitations and applying a best-fit model approach, we argue that our estimates of future CSL change based on CMIP6 models can be regarded as a state-of-the-art assessment to serve as a base for adaptation and mitigation measures.

Decrease in the lake surface area due to CSL decline will increase the A_T/A_S ratio applied in Eq. (1), thereby increasing the ΔCSL change. On the other hand, shrinking of the lake will also reduce the evaporation over the Caspian Sea. Changes in the intensity of Caspian Sea gyres and the resulting effects on heat mixing can further influence the evaporation rate from the Caspian Sea surface[36]. Therefore, future studies should consider the coupling of dynamical lake models with climate models to correctly incorporate bathymetry of the Caspian Sea, changes in the lake surface area, and lake-climate feedbacks. Taking those processes into account will likely reduce uncertainties in future CSL projections. Moreover, future studies can focus on simulating regional hydroclimate using high-resolution regional climate models. It should finally also be noted that direct anthropogenic influences like irrigation and dam building were not taken into account in this study either. Changes to regional population, land-use change, and effective water utilization resulted in a reduction in water extraction in the last few decades[39]. However,

this reduction was not adequate enough to balance the effect of evaporation over the Caspian Sea resulting in further CSL decline[10]. Water withdrawals will have an impact on the future CSL even though improvements in water consumption are expected[8]. Water extraction will therefore most likely result in further CSL decline in addition to the estimated drop due to increasing temperature.

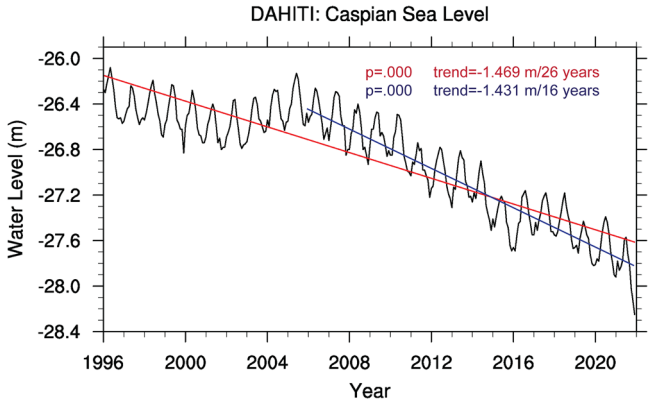

Fig. 7 Trend analysis of CSL timeseries of DAHITI data based on satellite altimetry for the time period 1996–2021. Data from ref. [55] (https://dahiti.dgfi.tum.de/en/39/).

Methods

CMIP6 model data description. Datasets from CMIP6 global climate model output were retrieved from the CMIP6 search interface of the World Climate Research Programme hosted by Deutsches Klimarechenzentrum. For our analysis, 15 models from 13 institutions with complete datasets were used (Table 1). Complete datasets include four variables (*P*, *E* including sublimation and transpiration, 2 m air temperature T2m, wind speed) for historical runs of the 1850–2014 period and future projections data of the 2015–2100 period (ScenarioMIP) for three Shared Socioeconomic Pathways (SSPs), viz SSP126, SSP245, and SSP585. Only first ensemble members 'r1i1p1f1' were considered. The Caspian Sea is implemented as an ocean in 5 models while the others simulate it by a simple lake parameterization. All the CMIP6 models have nominal resolution of 100 km.

Reanalysis data. ERA5 data with high spatial resolution of 0.25° x 0.25° were retrieved from the Copernicus Climate Change Service Climate Data Store[40]. The historical simulations of CMIP6 that span over the period of 1850–2014 were applied for a

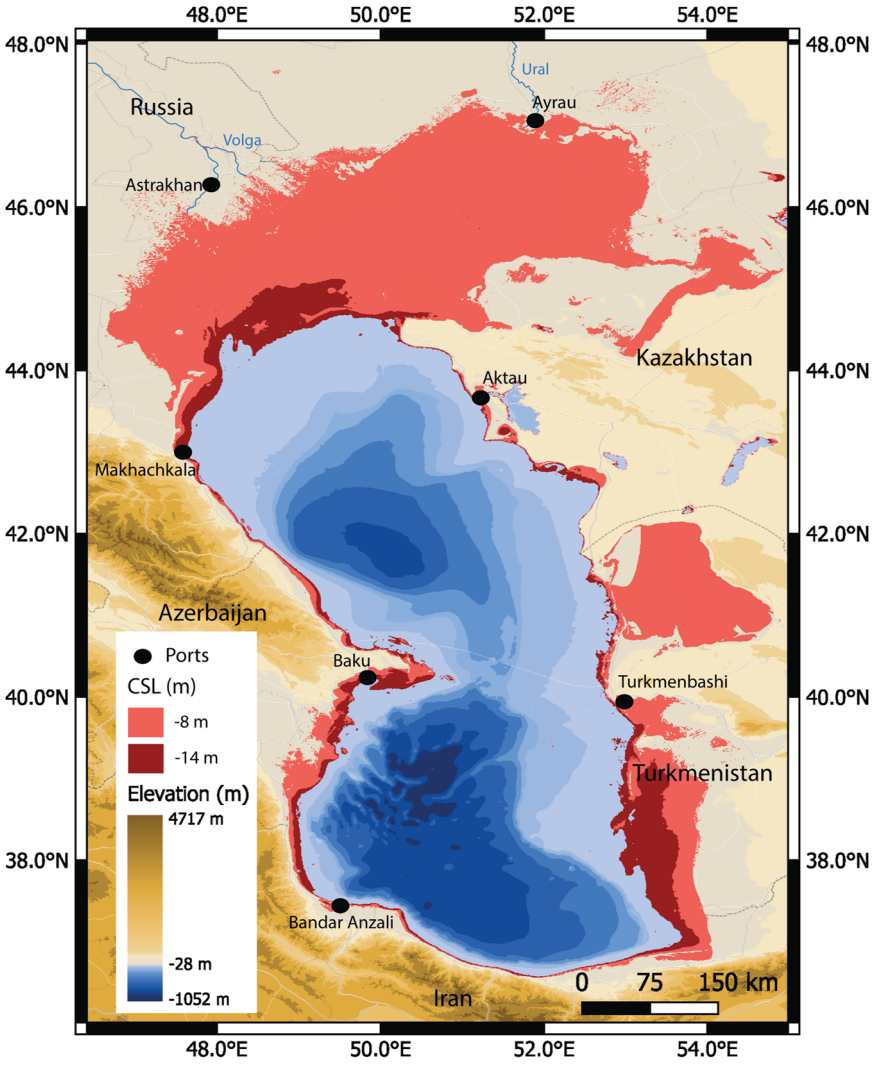

Fig. 8 Impact on the Caspian Sea for a projected decline of 8–14 m by the end of the 21st century for SSP245 and SSP585, respectively. Red regions show drying.

comparative analysis with a focus on the catchment region of the Caspian Sea, i.e., 36–60°N, 45–55°E. This comparison for the period 1979–2008 was vital to identify precipitation, evaporation, and temperature biases in the simulations and, thus, offered insights into the ability of the models to simulate the climate of the Caspian region.

Data processing and analysis. Annual mean values weighted and averaged over the precisely masked Caspian catchment area and sea surface area were calculated and used to carry out linear trend analyzes for precipitation, evaporation, air temperature, and wind speed. SSP126, SSP245, and SSP585 scenarios of the CMIP6 future simulations were analyzed over the interval 2020–2100. To estimate the future changes in CSL, linear trends of $P–E$ were evaluated. Trend analysis was carried out using linear regression. Results are given with 95% confidence intervals for the regression slopes. Other inter-model uncertainties (historical $P–E$ means, standard deviations) are reported in the figures and in supplementary information. All analyzes were performed using the National Center for Atmospheric Research Command Language.

Data availability

The CMIP6 model datasets processed and analyzed in this study were retrieved from the CMIP6 search interface of World Climate Research Programme (https://esgf-data.dkrz.de/search/cmip6-dkrz/) hosted by Deutsches Klimarechenzentrum. The ERA5 data implemented in this work is available at the Copernicus Climate Change Service Climate Data Store (https://cds.climate.copernicus.eu/#!/search?text=ERA5&type=dataset). The bathymetry data were acquired from GEBCO Compilation Group (2022) GEBCO 2022 Grid while the satellite altimetry data is available at the Database for Hydrological Time Series of Inland Waters (DAHITI) (https://dahiti.dgfi.tum.de/en/39/).

Received: 24 March 2023; Accepted: 20 September 2023;
Published online: 07 October 2023

References

1. Pörtner, H.-O. et al. Climate change 2022: Impacts, adaptation and vulnerability. In *IPCC Sixth Assessment Report* (IPCC, 2022).
2. Prange, M., Wilke, T. & Wesselingh, F. P. The other side of sea level change. *Commun. Earth Environ.* **1**, 1–4 (2020).
3. Wang, J. et al. Recent global decline in endorheic basin water storages. *Nat. Geosci.* **11**, 926–932 (2018).
4. Winter, T. C. in *Physics and Chemistry of Lakes* 37–62 (Springer, 1995).
5. Healy, R. W., Winter, T. C., LaBaugh, J. W. & Franke, O. L. *Water Budgets: Foundations for Effective Water-Resources and Environmental Management* (US Geological Survey Reston, Virginia, 2007).
6. Hollis, G. The falling levels of the Caspian and Aral Seas. *Geogr. J.* **144**, 62–80 (1978).
7. Mischke, S. *Large Asian Lakes in a Changing World: Natural State and Human Impact* (Springer Nature, 2020).
8. Koriche, S. A., Singarayer, J. S. & Cloke, H. L. The fate of the Caspian Sea under projected climate change and water extraction during the 21st century. *Environ. Res. Lett.* **16**, 094024 (2021).
9. Arpe, K. et al. Connection between Caspian sea level variability and ENSO. *Geophys. Res. Lett.* **27**, 2693–2696 (2000).
10. Chen, J. et al. Long-term Caspian sea level change. *Geophys. Res. Lett.* **44**, 6993–7001 (2017).
11. Akbari, M. et al. Vulnerability of the Caspian Sea shoreline to changes in hydrology and climate. *Environ. Res. Lett* **15**, 115002 (2020).
12. Pekel, J.-F., Cottam, A., Gorelick, N. & Belward, A. S. High-resolution mapping of global surface water and its long-term changes. *Nature* **540**, 418–422 (2016).
13. Elguindi, N. & Giorgi, F. Simulating future Caspian Sea level changes using regional climate model outputs. *Clim. Dyn.* **28**, 365–379 (2007).
14. Arpe, K. et al. Analysis and modeling of the hydrological regime variations in the Caspian Sea basin. in *Doklady Earth Sciences* 552–556 (Springer, 1999).
15. Elguindi, N. & Giorgi, F. Projected changes in the Caspian sea level for the 21st century based on the latest AOGCM simulations. *Geophys. Res. Lett* **33**, L08706 (2006).
16. Elguindi, N. & Giorgi, F. Simulating multi-decadal variability of Caspian sea level changes using regional climate model outputs. *Clim. Dyn.* **26**, 167–181 (2006).
17. Kislov, A. & Toropov, P. East European river runoff and Black Sea and Caspian Sea level changes as simulated within the paleoclimate modeling intercomparison project. *Quat. Int.* **167**, 40–48 (2007).
18. Renssen, H. et al. Simulating long-term Caspian sea level changes: the impact of holocene and future climate conditions. *Earth Planet. Sci. Lett.* **261**, 685–693 (2007).
19. Kislov, A., Panin, A. & Toropov, P. Current status and palaeostages of the Caspian Sea as a potential evaluation tool for climate model simulations. *Quat. Int.* **345**, 48–55 (2014).
20. Efimov, V., Volodin, E., Anisimov, A. & Barabanov, V. Regional projections of climate change for the Black Sea–Caspian Sea area in late 21st century. *Phys. Oceanogr.* **49**, 66 (2015).
21. Arpe, K. & Leroy, S. A. The Caspian Sea level forced by the atmospheric circulation, as observed and modelled. *Quat. int.* **173**, 144–152 (2007).
22. Roshan, G., Moghbel, M. & Grab, S. Modeling Caspian Sea water level oscillations under different scenarios of increasing atmospheric carbon dioxide concentrations. *Iran. J. Environ. HealthSci. Eng.* **9**, 1–10 (2012).
23. Nandini-Weiss, S. D., Prange, M., Arpe, K., Merkel, U. & Schulz, M. Past and future impact of the winter North Atlantic Oscillation in the Caspian Sea catchment area. *Int. J. Clim.* **40**, 2717–2731 (2020).
24. Arpe, K., Tsuang, B.-J., Tseng, Y.-H., Liu, X.-Y. & Leroy, S. A. Quantification of climatic feedbacks on the Caspian sea level variability and impacts from the Caspian sea on the large-scale atmospheric circulation. *Theoret. Appl. Clim.* **136**, 475–488 (2019).
25. Koriche, S. A. et al. Impacts of variations in Caspian sea surface area on catchment-scale and large-scale climate. *J. Geophys. Res. Atmos.* **126**, e2020JD034251 (2021).
26. Kosarev, A. N., Kostianoy, A. G. & Zonn, I. S. Kara-Bogaz-Gol Bay: physical and chemical evolution. *Aqua. Geochem.* **15**, 223–236 (2009).
27. Rodionov, S. *Global and Regional Climate Interaction: the Caspian Sea Experience* (Springer Science & Business Media, 1994).
28. Ivkina, N., Naurozbayeva, Z. & Kløve, B. Influence of climate change on the ice regime of the Caspian Sea. *Cent. Asian J. Water Res.* **3**, 12–23 (2017).
29. Kuprin, P. Apsheron threshold and its role in the processes of sedimentation and formation of hydrological regimes in the southern and middle Caspian basins. *Water Resour.* **29**, 473–484 (2002).
30. Kostianoy, A. G. & Kosarev, A. N. *The Caspian Sea Environment* (Springer Science & Business Media, 2005).
31. Kroonenberg, S. B., Kasimov, N. S. & Lychagin, M. Y. The Caspian Sea, a natural laboratory for sea-level change. *Geograp. Environ. Sustain.* **1**, 22–37 (2008).
32. Taylor, K. E. Summarizing multiple aspects of model performance in a single diagram. *J. Geophys. Res. Atmos.* **106**, 7183–7192 (2001).
33. Tokarska, K. B. et al. Past warming trend constrains future warming in CMIP6 models. *Science Adv.* **6**, eaaz9549 (2020).
34. Meehl, G. A. et al. Context for interpreting equilibrium climate sensitivity and transient climate response from the CMIP6 Earth system models. *Sci. Adv.* **6**, eaba1981 (2020).
35. Scafetta, N. Advanced testing of low, medium, and high ECS CMIP6 GCM simulations versus ERA5-T2m. *Geophys. Res. Lett.* **49**, e2022GL097716 (2022).
36. Huang, L., Lee, S.-S. & Timmermann, A. Caspian sea and black sea response to greenhouse warming in a high-resolution global climate model. *Geophys. Res. Lett.* **48**, e2020GL090270 (2021).
37. Wang, W. et al. Global lake evaporation accelerated by changes in surface energy allocation in a warmer climate. *Nature Geosci.* **11**, 410–414 (2018).
38. Yao, F. et al. Satellites reveal widespread decline in global lake water storage. *Science* **380**, 743–749 (2023).
39. Demin, A. Present-day changes in water consumption in the Caspian Sea basin. *Water Res.* **34**, 237–253 (2007).
40. Hersbach, H. et al. ERA5 monthly averaged data on single levels from 1979 to present. *Copernicus Clim. Chang. Serv. (C3S) Clim. Data Store (CDS)* **10**, 252–266 (2019).
41. Semmler, T. et al. Simulations for CMIP6 with the AWI climate model AWI-CM-1-1. *J. Adv. Model. Earth Syst.* **12**, e2019MS002009 (2020).
42. Wu, T. et al. The Beijing Climate Center Climate System Model (BCC-CSM): the main progress from CMIP5 to CMIP6. *Geosci. Model Dev.* **12**, 1573–1600 (2019).
43. Xin-Yao, R. et al. Introduction of CAMS-CSM model and its participation in CMIP6. *Adv. Clim. Chang. Res.* **15**, 540 (2019).
44. Cherchi, A. et al. Global mean climate and main patterns of variability in the CMCC-CM2 coupled model. *J. Adv. Model. Earth Syst.* **11**, 185–209 (2019).
45. Döscher, R. et al. The EC-Earth3 Earth system model for the climate model intercomparison project 6. *Geosci. Model Dev. Discuss.* **1**, 2021 (2021).
46. HE, B. et al. CAS FGOALS-f3-L model dataset descriptions for CMIP6 DECK experiments. *Atmos. Oceanic Sci. Lett.* **13**, 582–588 (2020).
47. Bao, Y., Song, Z. & Qiao, F. FIO-ESM version 2.0: model description and evaluation. *J. Geophys. Res. Oceans* **125**, e2019JC016036 (2020).
48. Dunne, J. et al. The GFDL Earth System Model version 4.1 (GFDL-ESM 4.1): overall coupled model description and simulation characteristics. *J. Adv. Model. Earth Syst.* **12**, e2019MS002015 (2020).

49. Volodin, E., Diansky, N. & Gusev, A. Simulation and prediction of climate changes in the 19th to 21st centuries with the Institute of Numerical Mathematics, Russian Academy of Sciences, model of the Earth's climate system. *Izv. Atmos. Ocean. Phys.* **49**, 347–366 (2013).
50. Volodin, E. et al. Simulation of modern climate with the new version of the INM RAS climate model. *Izv. Atmos. Ocean. Phys.* **53**, 142–155 (2017).
51. Müller, W. A. et al. A higher-resolution version of the Max Planck Institute Earth System Model (MPI-ESM1. 2-HR). *J. Adv. Model. Earth Syst.* **10**, 1383–1413 (2018).
52. Yukimoto, S. et al. The Meteorological Research Institute Earth System Model version 2.0, MRI-ESM2. 0: description and basic evaluation of the physical component. *J. Meteorol. Soc. Japan. Ser. II* **97**, 931–965 (2019).
53. Seland, Ø. et al. Overview of the Norwegian Earth System Model (NorESM2) and key climate response of CMIP6 DECK, historical, and scenario simulations. *Geosci. Model Dev.* **13**, 6165–6200 (2020).
54. Lee, W.-L. et al. Taiwan Earth system model version 1: description and evaluation of mean state. *Geosci. Model Dev.* **13**, 3887–3904 (2020).
55. Schwatke, C., Dettmering, D., Bosch, W. & Seitz, F. DAHITI–an innovative approach for estimating water level time series over inland waters using multi-mission satellite altimetry. *Hydrol. Earth Syst. Sci.* **19**, 4345–4364 (2015).

Acknowledgements

We are grateful to Andreas Manschke for his technical support. M.P. was supported by the project PRIDE (Pontocaspian RIse and DEmise) which has received funding from the European Union's Horizon 2020 research and innovation program. We thank two anonymous reviewers for their constructive reviews and suggestions on the manuscript.

Author contributions

Manuscript concept was developed by R.S. and M.P., manuscript was written by R.S. and M.P., data processing and analysis was performed by R.S. and M.P., figures were made by R.S.

Funding

Open Access funding enabled and organized by Projekt DEAL.

Competing interests

The authors declare no competing interests.

Additional information

Supplementary information The online version contains supplementary material available at https://doi.org/10.1038/s43247-023-01017-8.

Correspondence and requests for materials should be addressed to Rohit Samant or Matthias Prange.

Peer review information *Communications Earth & Environment* thanks the anonymous reviewers for their contribution to the peer review of this work. Primary Handling Editors: Mengze Li, Heike Langenberg. A peer review file is available.